Electronic Supplementary Material (ESI) for Soft Matter.

Supporting information for

Role of Solvent Swelling in Self-Assembly of Squalene based Nanomedicines

Debasish Saha,[a] Fabienne Testard,[a] Isabelle Grillo,[b] Fatima Zouhiri,[c] Didier Desmaele,[c] Aurel Radulescu,[d] Sylvain Desert,[e] Annie Brulet,[e] Patrick Couvreur [c] and Olivier Spalla *[a]

[a]CEA Saclay, DSM/IRAMIS/NIMBE/LIONS, UMR CEA/CNRS 3299, 91191 Gif sur Yvette, France
[b]Institut Laue-Langevin, BP 156, 38042 Grenoble Cedex 9, France
[c]Université Paris-Sud, UMR CNRS 8612, Faculté de Pharmacie, Châtenay-Malabry, F-92296, France
[d]Jülich Centre for Neutron Science JCNS, Forschungszentrum Jülich GmbH,Outstation at MLZ, Lichtenbergstraße 1, 85747 Garching, Germany
[e] Laboratoire Léon Brillouin UMR12 CEA-CNRS, Bât 563 CEA Saclay, 91191 Gif sur Yvette Cedex, France

I. Composition of samples

The detail of the composition for all tested nanoparticles is listed in Table S1. .

Table S1: Composition of the *intermediate* and *final states* of deoxycytidine squalene, squalenic acid and gemcitabine squalene nanoparticles and Table S1 total concentration C_f.

Sample	C_i (mg/mL)[a]	Φ_{D2O} (%v/v)[b]	Φ_{ETOH} (%v/v)[c]	C_f (mg/mL)[d]	Corresponding figure for the sample
CSE1	5.48	0.991	0.009	0.07	Fig 3A
CSE2	5.48	0.863	0.070	0.52	Fig 3A
CSE3	5.48	0.898	0.102	0.75	Fig 3A
CSE4	5.48	0.869	0.131	0.96	Fig 3A
CSE5	5.48	0.816	0.184	1.32	Fig 3A
CSE6	5.48	0.769	0.231	1.62	Fig 3A
SAE1	6.70	0.932	0.068	0.63	Fig S1A
SAE2	6.70	0.853	0.147	1.31	Fig S1A
SAE3	6.70	0.697	0.303	2.55	Fig S1A
GSE1	4.15	0.919	0.081	0.41	Fig S2
GSE2	4.15	0.873	0.127	0.64	Fig S2
GSE3	4.15	0.818	0.182	0.90	Fig S2
GSE4	4.15	0.604	0.396	1.86	Fig S2
CS1	6.38	0.898	0.102	2.08	Fig 3B
CS2	6.38	0.884	0.116	2.59	Fig 3B
CS3	6.38	0.874	0.126	3.73	Fig 3B
SA1	6.64	0.930	0.070	1.91	Fig S1B
SA2	6.64	0.805	0.195	4.06	Fig S1B
SA3	6.64	0.786	0.214	6.74	Fig S1B
GS1	4.20	0.856	0.144	1.83	Fig 4
GS2	4.20	0.827	0.173	2.01	Fig 4
GS3	4.20	0.799	0.201	2.77	Fig 4
GS4	4.20	0.784	0.216	3.01	Fig 4

[a]Initial concentration of squalene derivative in ethanol; CSE, SE, CS, SA and GS series samples were prepared using protonated ethanol while GSE series samples were prepared using deuterated ethanol [b]Mass fraction of D_2O in the solvent, [c]Mass fraction of ethanol in the solvent,

mass fractions were calculated from initial composition for intermediate sample and issued from SANS background analysis for final ones. [d] Total squalene derivative concentration. Total concentrations were calculated from the initial weight for the intermediate sample and from UV-visible for final one.

II. SANS acquisition conditions

SANS experiments were carried out on the D22 spectrometer at ILL, KWS-2 spectrometer at FRMII, PAXY and TPA spectrometers at LLB.

For ILL measurement on the D22 spectrometer, all the samples were put in 1 mm HELLMA cells and aligned using the thermostatic sample holder with a temperature control of 20 °C. All the measurements were done at λ = 11.5 Å. Three different settings were used for this experiment to cover q-range from $1.5*10^{-3}$ to 0.3 $Å^{-1}$. The detector distances 17.0 m, 5.0 m and 1.3 m and the collimations 17.6 m, 8.0 m and 5.6 m were used respectively for the small angle (SA), middle angle (MA) and large angle (LA). The raw data were radial averaged, corrected for electronic background and empty cell and normalized by water scattering using the LAMP software.

For the FRMII measurement at KWS2 spectrometer, two different wavelengths were used to cover from large angle to ultra-small angle. The collimator distance of 8.0 m and 20.0 m and the detector distance of 1.66m, 7.66m and 19.66 m were used at λ = 5.3 Å to cover the LA-MA-SA range ($7*10^{-4}$ $Å^{-1}$ to 0.3 $Å^{-1}$). In order to reach the ultra-small angle region (up to q = $7*10^{-4}$ $Å^{-1}$), a special feature of this instrument was utilized. At very large wavelength (λ = 17.7 Å), where the intensity of neutrons are very low, the beam stop has been removed and the direct beam was measured to cover the ultra-small angle region. The raw data were radial averaged, corrected for electronic background and empty cell and normalized by water scattering using the qtiKWS software.

For the LLB measurements, data obtained from two different spectrometers (PAXY and TPA) have been scaled in absolute value and merged together to cover from large angle to ultra small angle. At PAXY, two different wavelengths were used (λ = 5.0 and 12.0 Å) to cover a q range from $2*10^{-3}$- 0.25 $Å^{-1}$, while at TPA three wavelengths have been used (λ = 6.0, 9.0 and 12.0 Å) to cover a q-range from $5*10^{-4}$- $5*10^{-3}$ $Å^{-1}$. The raw data obtained from both instruments were treated and reduced to absolute scattering units by using the Pasinet software.

III. SQ-CO2H nanoparticles:

SANS spectra of the intermediate states are shown in Fig. S1A and the final states are in Fig. S1B. Nanoparticles forms as revealed by a Porod behavior at large q observed both for the intermediate states and final states. However, on the contrary to deoxycytidine squalene and gemcitabine squalene cases, squalenic acid nanoparticles do not present internal structure neither in the intermediate states nor in the final states. In the low q range, the trace of Guinier regime is obtained only at very low concentration of intermediate states and completely disappeared with increasing concentration. Moreover, the impact of the evaporation stage to produce "final states" was completely opposite to the deoxycytidine squalene case. There was no trace of a Guinier regime telling that the particles were much bigger than what could be measured. Aggregation and coalescence of squalenic acid nanoparticles occurred during the evaporation stage. Samples were however stable long enough to be measured by SANS afterwards.

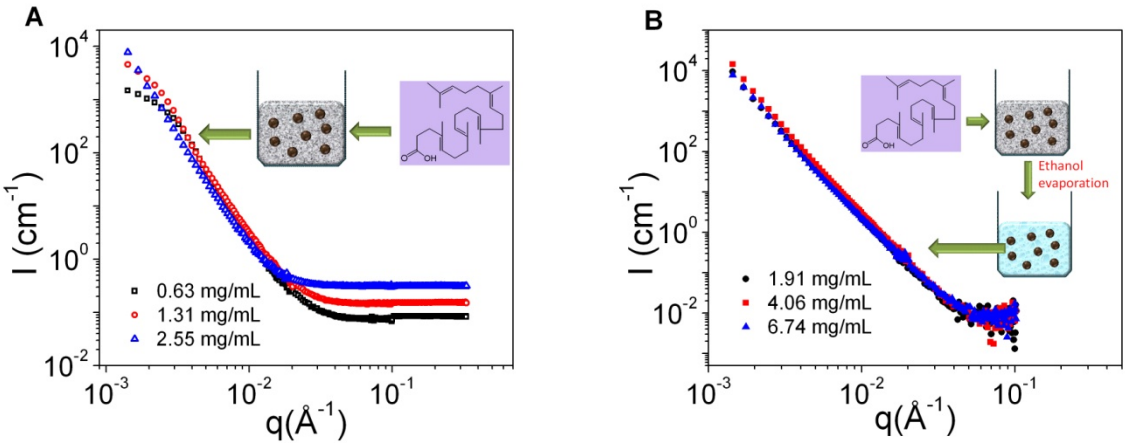

Fig. S1: (A) SANS (ILL) patterns of the intermediate state of squalenic acid nanoparticles obtained during the drop by drop addition of ethanolic solution (6.70 mg/ml) into D_2O. (B) SANS patterns of the final state of squalenic acid nanoparticles at different concentrations obtained by drop by drop addition.

IV. Contrast of scattering length density:

Swelling by solvent: considering the swelling factor $\alpha = \Phi_{tot} / \Phi_{Sq}$, the *solvent* volume fraction in the particles was calculated: $\Phi_{Solvent}^{nanoparticles} = 1 - \frac{1}{\alpha}$ allowing calculation of the scattering length density of the nanoparticles $\rho = \left(1 - \frac{1}{\alpha}\right) \times \rho_{Sol} + \left(\frac{1}{\alpha}\right) \times \rho_{Sq}$.

Swelling by ethanol: considering the swelling factor $\alpha = \Phi_{tot} / \Phi_{Sq}$, the *ethanol* volume fraction in the particles was calculated: $\Phi_{EtOH}^{nanoparticles} = 1 - \frac{1}{\alpha}$ allowing calculation of the scattering length density of the nanoparticles $\rho = \left(1 - \frac{1}{\alpha}\right) \times \rho_{EtOH} + \left(\frac{1}{\alpha}\right) \times \rho_{Sq}$.

Swelling by water: considering the swelling factor $\alpha = \Phi_{tot} / \Phi_{Sq}$, the *water* volume fraction in the particles was calculated: $\Phi_{D_2O}^{nanoparticles} = 1 - \frac{1}{\alpha}$ allowing calculation of the scattering length density of the nanoparticles $\rho = \left(1 - \frac{1}{\alpha}\right) \times \rho_{D_2O} + \left(\frac{1}{\alpha}\right) \times \rho_{Sq}$.

In order to calculate the exact scattering length density of the solvent in the *intermediate states* the background of the SANS spectra has been used to extract the unknown volume fraction of ethanol and D_2O after solvent evaporation. Knowing the contrast term, the number density of particles could be extracted from $N(\Delta\rho)^2$. The total SANS volume fraction of scattered particles was then obtained by the $N \times V_{tot}$ product.

V. Measure of the D_2O/EtOH ratio by mean of the background at large angle.

In the large q range, the background was increasing with increasing the number of drops which was related to the increasing of ethanol content. The solvent, D_2O/Ethanol composition could be accessed directly by the level of incoherent background at large q when the ethanol molecule was protonated contrary to D_2O. Indeed, the observed backgrounds were larger than pure D_2O signal

(0.026 cm^{-1}). For the intermediate states, the increase of the background with increasing the number of added drop was related to the increase amount of ethanol in the solution which contributed to an increase of incoherent background of scattering. The concentration of squalene derivatives being negligible as compared to the ethanol, therefore its contribution in the background could be neglected.

For *final states* from which in an ideal case ethanol should have been fully evaporated, it is expected to measure an identical background to D_2O for all. In practice, the scenario was more complex and not only higher but also different backgrounds have been obtained for different *final states*. This was a clear indication of the presence of residual ethanol in the *final state* since the low amount of squalene derivatives in the solution (~2.0-3.8 mg/mL) could not explain this difference. The amount of residual ethanol could be retrieved by a quantitative analysis of the experimental background level scaled in the absolute unit.[1] The incoherent scattering level for pure solvents i.e. ethanol, H_2O, D_2O and mixture of solvents have been measured in the absolute scale at large angle by neutron scattering. This yielded a straight line, while the background for the different solvents was plotted as a function of hydrogen fraction. Therefore, the background from the different final states could be taken as a linear superposition of the D_2O fraction and the ethanol fraction. In principal, the incoherent background of different final states could be formulated in the following way:

$$\Sigma_{incoherent,sample} = \phi_{D_2O} \Sigma_{incoherent,D_2O} + \phi_{ethanol} \Sigma_{incoherent,ethanol}$$

where, $\Sigma_{incoherent,sample}$ is obtained from the backgrounds of final states while and $\Sigma_{incoherent,D_2O}$ $\Sigma_{incoherent,ethanol}$ are obtained from the background of pure D_2O and pure ethanol. ϕ_{D_2O} and $\phi_{ethanol}$ are respectively the volume fraction of D_2O and ethanol in the final states. The analysis revealed a finite value of residual ethanol (around 10 to 15%v/v) in the final states. This is a clear

indication of i) the presence of residual ethanol even after final evaporation and ii) a finite amount of D_2O co-evaporated together with ethanol. This was leading to a mismatch between weight decrease and ethanol content decrease.

VI. *Intermediate state* with Gemcitabine using deuterated ethanol

In order to reduce the background due to hydrogens atoms, we used deuterated ethanol (C_2D_5OD) for the precipitation of the *intermediate states of* gemcitabine squalene nanoparticles. In addition, the use of deuterated ethanol allowed increasing the stability of these intermediate states in comparison to protonated ethanol although these samples were demixed after few days. As reported in Fig. S2, two oscillations in a log-log plot of the scattered intensity were observed in the Porod regime for the low concentrations up to C = 0.90 mg/mL. These oscillations were the signature of monodisperse particles. Further increase in concentration turned the monodisperse particles into polydisperse ones. This feature was opposite to the intermediate states of deoxycytidine squalene nanoparticles where no oscillation was present even for the lowest experimental concentration (C = 0.07 mg/mL). In the Porod regime, the signal decreased with a power law of q^{-4} in the q range ~ 0.008 $Å^{-1}$ to 0.025 $Å^{-1}$ for the smallest concentration in the *intermediate states*, revealing an abrupt interface between the nanoparticles and the solvent at the scale of a few nanometers.[2] This Porod regime drastically shifted to lower q, while the concentration lifted up from 0.90 mg/mL to 1.86 mg/mL. This was a signature of bigger particle formation at higher concentrations.

The saturation regime could be attained up to C = 0.90 mg/mL. A Guinier analysis of the signal at low q indicated that nanoparticles were quite small ~ 75 nm at lowest experimental concentration (C = 0.41 mg/mL). The upturn at low q got higher with increasing concentration revealing that particles were getting bigger.

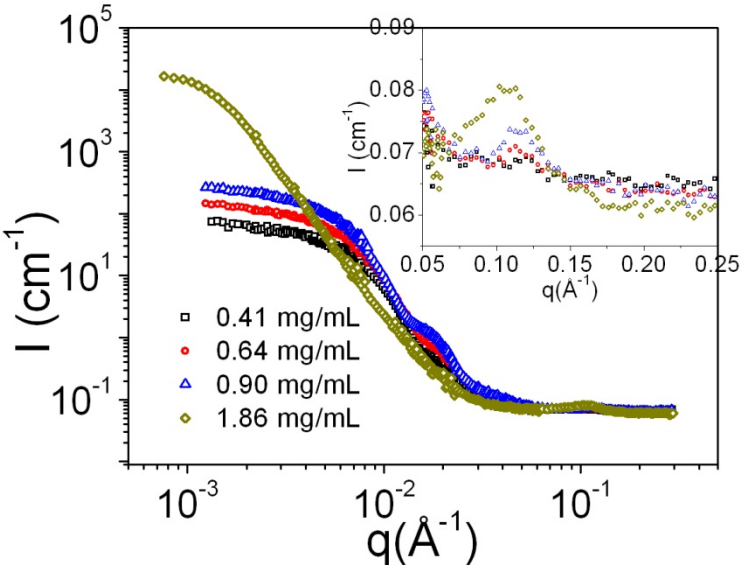

Fig. S2. SANS patterns (FRMII, KWS2) of the intermediate state of gemcitabine squalene nanoparticles obtained during the drop by drop addition of d-ethanol solution into D_2O. In inset, a zoom at wide angle shows the apparition and variation of a Bragg peak.

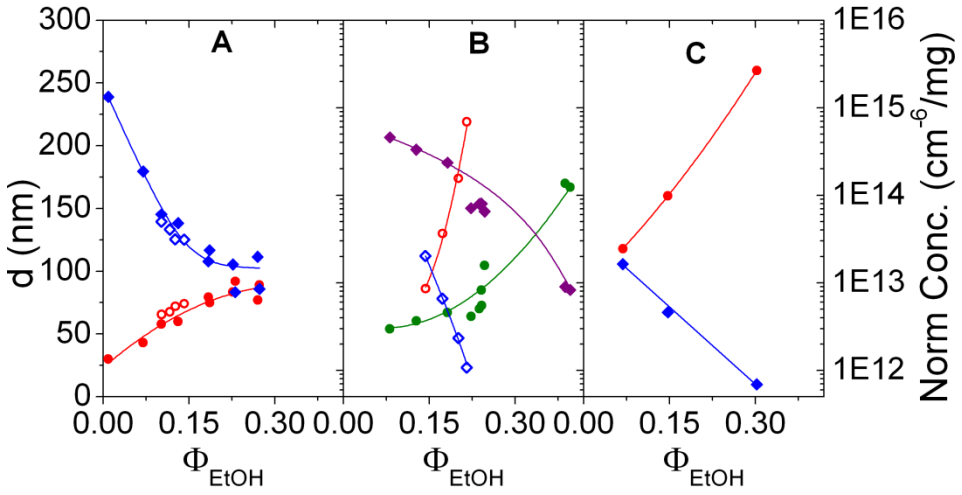

Fig. S3. Diameter (nm) and normalized number density (cm^{-3}/mg) versus ethanol fraction in solvent for *intermediate states* (filled symbols) and *final states* (empty symbols). Circles stand for diameters and diamonds stand for number density. A) Deoxycytidine squalene B) Gemcitabine squalene (green and purple symbols are *intermediate states* nanoparticles made with deuterated ethanol). C) Squalenic acid.

VII. Concentration measurement of the *final states* by UV spectroscopy:

The concentrations for the intermediate states were easy to determine from the weight-measurement by high precision balance. But the scenarios were completely different for the final states after the organic solvent evaporation. The classical solvent elimination techniques are not accurate to remove the organic solvent completely without any elimination of the non-solvent. Either a considerable amount of ethanol left or a small amount of D_2O evaporated together with ethanol or both scenarios simultaneously took place during the solvent evaporation. Therefore, the solvent evaporation yields final state for which the composition and concentration is completely unknown. The weight measurements cannot produce the proper concentration any more for the final state. Therefore, the UV spectroscopy has been used to measure the concentration of the final states of nanoparticles by diluting the samples in absolute ethanol (>99.8%). Using Beer-Lambert law and calibration curves of squalenoyl derivative in ethanol, we extracted the precise composition for each sample at the final state.

The wavelength range was chosen from 190 nm to 900 nm and samples were measured in a single Hellma UV quartz cell thickness of 1 mm.

For SQ-dC diluted in ethanol, three absorption peaks were visible at λ = 300.5, 248.0 and 197.0 nm. The positions of the first and second peak were more precisely defined than the third peak. Therefore, only these first two absorbance peaks were taken for analysis. The absorbance spectra recorded for different concentrations are plotted in Fig. S4A with in inset, the calibration curves extracted for the two first peaks.

The molar absorptivity of SQ-dC was calculated as 668.7±11.8 from the first peak and 1352.6±11.8 from the second peak.

The final states of the nanoparticles with unknown concentration were highly diluted by ethanol at different dilution factors to fit with the concentration range of the calibration curves Representative UV-vis absorbance spectra of diluted samples are shown in Fig. S4B. In order to reduce the error, the concentration of the final state was taken as the average of different concentration obtained from several dilutions. The concentrations found by either 2nd peak or 1st peak intensities were in good agreement.

Similar procedure has been repeated for the *final state* of gemcitabine squalene and squalenic acid nanoparticles.

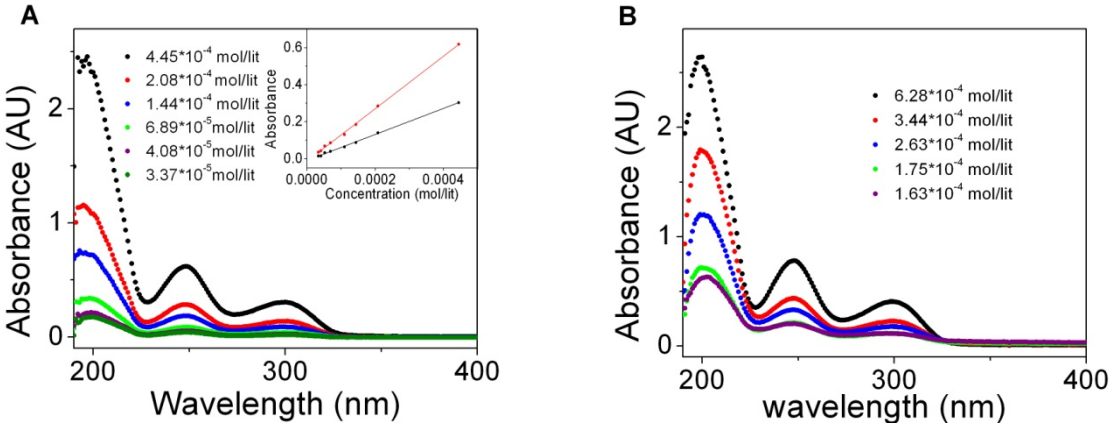

Fig. S4: The absorbance peaks of pure deoxycytidine squalene solution in ethanol at different dilution are plotted as a function of wavelength. The molar absorptivity is obtained from the absorbance vs. concentration plot. The absorbance peaks of the final state of nanoparticles in ethanol at different dilutions are plotted as a function of the wavelength. (A): Calibration curve only with deoxycytidine squalene molecules; (B): deoxycytidine squalene nanoparticles sample highly diluted in absolute ethanol.

REFERENCES

1 C. J. Glinka, *J. Appl. Crystallogr.*, 2011, **44**, 618–624.
2 O. Spalla, in *Neutron, X-rays and Light. Scattering Methods Applied to Soft Condensed Matter*, North-Holland, 1st Edition., 2002.